A kinematic model for the East African Rift

D.S. Stamps, E. Calais, E. Saria, C. Hartnady, J.-M. Nocquet, C.J. Ebinger,
R. Fernandes

A kinematic model for the East African Rift

D. Sarah Stamps,[1] Eric Calais,[1] Elifuraha Saria,[2] Chris Hartnady,[3] Jean-Mathieu Nocquet,[4] Cynthia J. Ebinger,[5] and Rui M. Fernandes[6]

[1] The kinematics of the East African Rift (EAR) is the least well-known of all major plate boundaries. Here, we show that present-day data (a GPS+DORIS geodetic solution and earthquake slip vectors) are consistent with 3.2 Myr-average spreading rates and transform-fault azimuths along the Southwest Indian Ridge and support a kinematic model that includes three subplates (Victoria, Rovuma, and Lwandle) between Nubia and Somalia. Continental rifting in the EAR appears to involve localized strain along narrow rift structures that isolate large lithospheric blocks. **Citation:** Stamps, D. S., E. Calais, E. Saria, C. Hartnady, J.-M. Nocquet, C. J. Ebinger, and R. M. Fernandes (2008), A kinematic model for the East African Rift, *Geophys. Res. Lett.*, *35*, L05304, doi:10.1029/2007GL032781.

1. Introduction

[2] Although the East African Rift (EAR; Figure 1), the divergent plate boundary between Nubia and Somalia, is often cited as a modern archetype for rifting and continental breakup, its current kinematics is the least well-known of all major plate boundaries. Prior kinematic studies from 3.2 Myr average spreading rates and transform azimuths [*Jestin et al.*, 1994; *Chu and Gordon*, 1999; *Lemaux et al.*, 2002; *Horner-Johnson et al.*, 2005] or present-day GPS measurements [*Sella et al.*, 2002; *Prawirodirdjo and Bock*, 2004; *Fernandes et al.*, 2004] have obtained significantly different Nubia-Somalia angular velocities. However, two recently published estimates, one based on a re-analysis of spreading rates and transform-fault azimuths along the Southwest Indian Ridge (SWIR) [*Horner-Johnson et al.*, 2007], the other on GPS data and earthquake slip vectors along the EAR [*Calais et al.*, 2006], now converge to similar results, with a Nubia-Somalia rotation pole located off the tip of South Africa and a rotation rate of 0.09 versus 0.07°/Myr, both within each others error bounds (Figure 1). These two studies also postulate the existence of additional plates (Victoria, Rovuma, Lwandle) between Somalia and Nubia.

[3] In this paper, we test the consistency between present-day data (an improved geodetic solution and earthquake slip vector data set) and 3.2 Myr average spreading date data along the SWIR and invert them jointly to derive an integrated kinematic model consistent with both data sets.

2. Data

2.1. Geodetic Solution

[4] The geodetic solution was obtained by combining four independent GPS solutions and one DORIS solution (Figure S1[1] and Table S3). The GPS data was processed in daily batches, then combined into a cumulative solution with position and velocity estimates. The GPS phase processing and pseudo-observable combination procedures are described, for instance, by *Nocquet et al.* [2006]. This cumulative solution was then combined with a DORIS solution [*Willis et al.*, 2005] to improve accuracy and spatial sampling over the study area. The International Terrestrial Reference Frame 2005 (ITRF2005) [*Altamimi et al.*, 2007] was applied by including the IGS cumulative solution IGS06P01 in the combination while minimizing position and velocity deviations of a globally distributed subset of stations (with velocity standard deviations <1 mm.yr^{-1}) from ITRF2005. We imposed in the combination that the velocity be the same at collocated DORIS and GPS sites. The agreement in horizontal velocities at sites common to several solutions, a measure of accuracy of the velocity field, is 0.6 mm.yr^{-1} (weighted RMS), with scaled uncertainties less than 1.5 mm.yr^{-1}.

2.2. Defining Stable Nubia

[5] Since the kinematic analysis will be conducted in a Nubia-fixed frame, we first seek to determine the subset of sites that best defines the rigid rotation of Nubia with respect to ITRF2005. We start by searching for the four sites whose velocity best matches a rigid rotation for Nubia. We then test each of the remaining sites one by one and quantify whether their velocity is consistent with the Nubia rotation defined by the best-fit, four-site subset. Ranking of four-site subsets and testing of additional sites are based on F-ratio, Student, and χ^2 tests [e.g., *Nocquet et al.*, 2006].

[6] This procedure shows that the best Nubia/ITRF2005 angular velocity (Table 1) is defined using sites ALEX, HRAO, MAS1, NKLG, PHLW, TGCV, YKRO, DAKA, HELA, TRIA, NSPT, IAVH, SIMO, and RBAY. The resulting reduced χ^2 is 1.5, with a weighted RMS of residual horizontal velocities of 0.7 mm.yr^{-1}, consistent with values found for other plate interiors. To further quantify the impact of the choice of sites that define Nubia, we compared the predicted velocity at MALI (Somalian plate) using all possible combinations of at least 8 sites among the 14 of our best-fit subset. We find a median

[1]Department of Earth and Atmospheric Sciences, Purdue University, West Lafayette, Indiana, USA.
[2]University College for Lands and Architectural Studies, University of Dar Es Salaam, Dar Es Salaam, Tanzania.
[3]Umvoto Africa Ltd., Cape Town, South Africa.
[4]CNRS Géosciences Azur, Valbonne, France.
[5]Department of Geology and Geophysics, University of Rochester, Rochester, New York, USA.
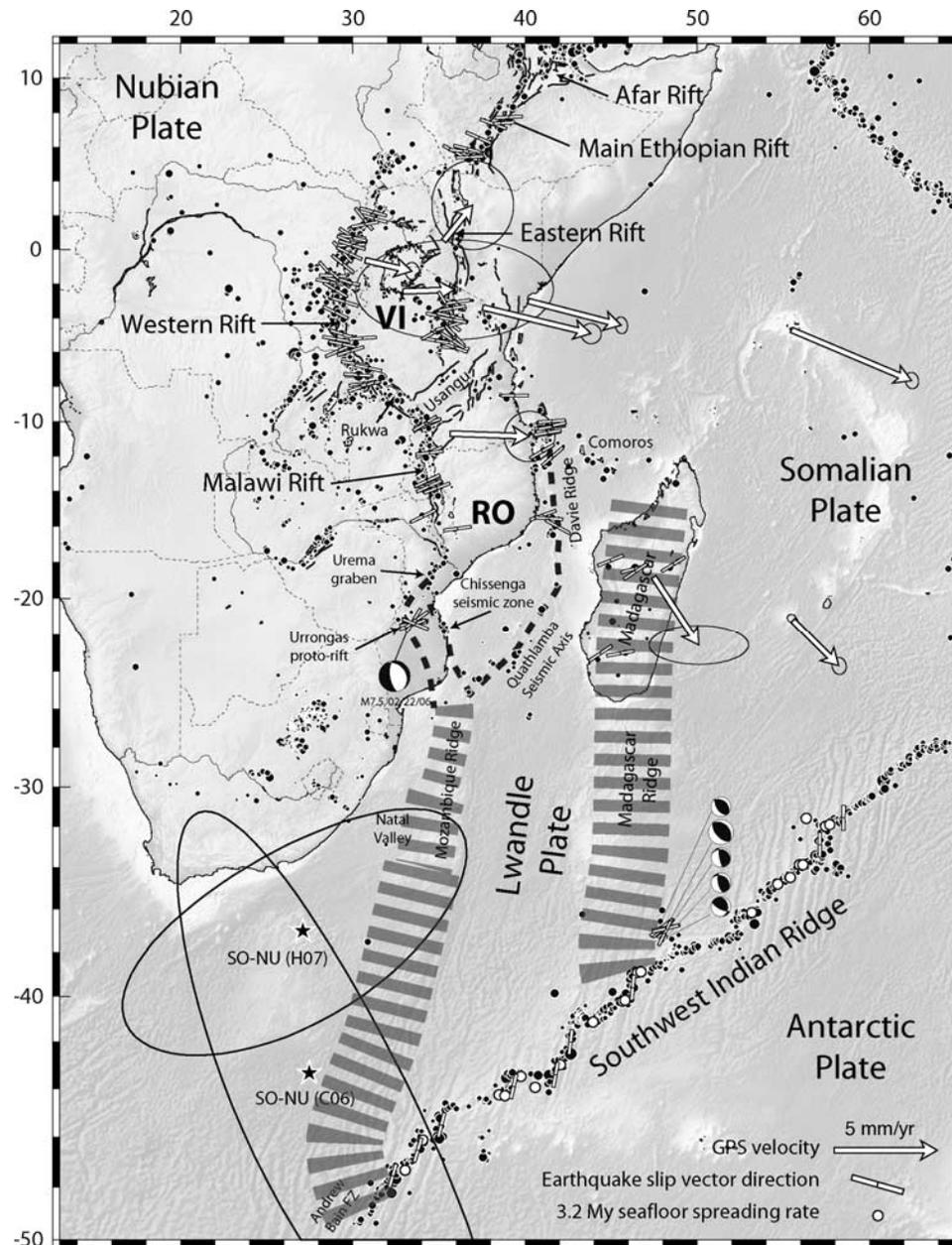[6]CGUL, IDL, UBI, Covilha, Portugal.

Figure 1. Seismotectonic setting of the East African Rift and data used. Solid black lines show major active faults [from *Skobelev et al.*, 2004], and small back circles show seismicity (NEIC catalog). Dashed lines indicate inferred plate boundary trace, and hatched area over Madagascar and the Madagascar ridge show the possibly diffuse Lwandle-Somalia plate boundary. Black stars indicate Nubia-Somalia rotation pole from *Calais et al.* [2006] and *Horner-Johnson et al.* [2007].

difference of 0.1 ± 0.2 mm.yr^{-1}, much smaller than the GPS velocity uncertainties.

2.3. Earthquake Slip Vectors

[7] We used the direction of earthquake slip vectors from the 53 focal mechanisms determined by *Foster and Jackson* [1998] and the 12 focal mechanisms determined by *Brazier et al.* [2005] from body-waveform inversion, augmented by the Global (Harvard) Centroid Moment Tensor (CMT) database (Table S2). We chose the same slip vectors as *Foster and Jackson* [1998], who based their choice on the structural framework of each epicentral region, and apply

the same criteria for the additional events. We used a conservative 20° uncertainty for all slip vectors.

[8] Earthquake slip vectors along the Ethiopian rift are assigned to the Nubia-Somalia plate boundary. South of about 3°N, the Ethiopian rift splits into the Western and Eastern rifts bounding the deep-rooted and relatively aseismic Tanzania craton. The plate boundary between those two branches at 4°N is complicated by Mesozoic rift structures; we use the boundary of *Ebinger* [1989] for simplicity. We assign earthquake slip vectors along the Western and Eastern branches to the Nubia-Victoria and Victoria-Somalia boundaries, respectively.

Table 1. Angular Velocity Estimates, With Associated Uncertainties, Chi-Squared, and Degrees of Freedom[a]

Test	Plate	Lat.	Lon.	S-maj.	S-min.	Azim.	Ang.	σ_{ang}
ITRF2005	NUBI	51.2445	−80.3948	4.1304	1.5583	86.2619	0.2441	0.0004
Final Solution	SOMA	−35.7195	35.2868	2.08	1.5	181.42	−0.0884	0.0044
	VICT	8.3696	32.5886	1.8	1	22.55	0.1294	0.0058
	ROVU	−30.1973	36.3305	3.26	1.54	180.96	−0.0991	0.0108
	ANTA	−2.2983	143.2710	2.16	1.02	31.19	0.1161	0.0018
	LWAN	−29.7274	1.0831	25.87	5.39	134.50	−0.0224	0.0065

[a]Angular velocities are in degree per million years, clockwise is positive. Azimuth is given clockwise from north. First table line gives Nubia angular velocity with respect to ITRF-2005 based on the best-fit subset of sites ALEX, HRAO, MAS1, NKLG, PHLW, TGCV, YKRO, DAKA, HELA, TRIA, NSPT, IAVH, SIMO, and RBAY.

[9] We assigned earthquake slip vectors along the Malawi rift to the Nubia-Rovuma boundary, which continues further south as a single belt of seismicity along the Shire and Urema grabens in Mozambique [*Hartnady*, 2006]. Earthquake slip vectors further south are available only for the 2006, M7.5 Mozambique earthquake and its main aftershocks [*Fenton and Bommer*, 2006], which we assign to the Nubia-Rovuma boundary as well.

[10] Earthquake slip vectors along the coast of Tanzania and northern Mozambique follow a well-defined belt of seismicity contiguous with active structures of the Davie ridge to the south [*Mougenot et al.*, 1986; *Grimison and Chen*, 1988]. We assign them to the Rovuma-Somalia boundary, although events on the southern part of the Davie ridge may in fact lie on the Rovuma-Lwandle boundary.

[11] The broad deformation zone encompassing the Madagascar Ridge and the island of Madagascar [*Kusky et al.*, 2007] may mark the Lwandle-Somalia boundary, with earthquake slip vectors in Madagascar (E−W extension) and near the southern end of the Madagascar ridge (NE−SW compression; Figure 1) representative of Lwandle-Somalia relative motion. This will be tested below.

[12] No earthquake slip vector is available along the poorly-defined Victoria-Rovuma and Rovuma-Lwandle boundaries. We tentatively draw the former along a belt of moderate seismicity, aligned eruptive centers, and recent faulting in the Usangu-Ruaha-Kilombero grabens [*Ebinger*, 1989; *Le Gall et al.*, 2004], and the latter along the Quathlamba Seismic Axis [*Hartnady*, 1990].

2.4. SWIR Data

[13] We use the spreading rates and transform fault azimuths along the SWIR and associated uncertainties from *Horner-Johnson et al.* [2005]. Following *Horner-Johnson et al.* [2007], the data are assigned to three separate segments of the SWIR: the Nubia-Antarctic plate boundary west of 29°E, the Lwandle-Antarctic plate boundary between 29°E and 47°E, and the Somalia-Antarctic plate boundary east of 47°.

3. Model

3.1. Methodology

[14] We model horizontal surface velocities as the result of rigid plate rotations. We neglect elastic strain accumulation on active faults as all geodetic sites used here are located more than 100 km away from major active structures. Plate boundary contours only serve to assign GPS velocities and earthquake slip vectors to the appropriate plate or pair of plates.

[15] We use Nubia as the reference plate for the geodetic solution and invert "geologic" data (3.2 Myr average spreading rates and transform azimuths along the SWIR) and "present-day" data (horizontal GPS velocities and earthquake slip vector directions) to solve for plate angular velocities while imposing plate circuit closure. We compare models using the F-ratio statistics to test the significance of the decrease in χ^2 from an estimate with p_2 degrees of freedom to an estimate with p_1 degrees of freedom ($p_1 > p_2$):

$$F = \frac{\left(\chi_{p_1}^2 - \chi_{p_2}^2\right)/(p_1 - p_2)}{\chi^2/p_2} \tag{1}$$

[16] This experimental F-ratio is compared to the expected value of a $F(p_1 - p_2, p_1)$ distribution for a given risk level $\alpha\%$ (or a 100-$\alpha\%$ confidence level) that the null hypothesis (the decrease in χ^2 is not significant) can be rejected [e.g., *Stein and Gordon*, 1984].

3.2. Tests Without Lwandle Plate

[17] We first compare two estimates of the Nubia-Somalia-Antarctica kinematics: one with the geologic data, and the other without (Table 1). We do not include a Lwandle plate and do not use geologic data along the Lwandle-Antarctica segment of the SWIR. Using the F-ratio statistics defined above, we find that the significance of the decrease in χ^2 from the estimate based on geologic and present-day data to the estimate based on present-day data alone is 1% (F = 0.66; Table S1). This implies that the two estimates are not statistically distinguishable and shows that the geologic and present-day data are consistent with each other within their uncertainties.

[18] The resulting Somalia-Nubia rotation pole falls within the 95% confidence ellipse of the *Horner-Johnson et al.* [2007] estimate (Figure S1). The same holds for the angular rotation rate (0.092 ± .012 versus 0.089 ± .005°/Myr). This new Somalia-Nubia angular velocity is different from that of *Calais et al.* [2006]: the 95% confidence ellipses of the rotation poles are close but do not overlap, and the new angular rotation rate is slightly faster (0.069 ± 0.013 versus 0.089 ± .005 °/Myr). The estimate based on present-day data only (Figure S1) shows a slightly different Somalia-Nubia angular velocity, still consistent with the *Horner-Johnson et al.* [2007] estimate and now consistent within 95% error bounds with that of *Calais et al.* [2006]. The difference between the new present-day plus geologic Somalia-Nubia angular velocity and that of *Calais et al.* [2006] therefore results from the inclusion of geologic data, but also from the use of a combined−and likely more accurate−GPS + DORIS
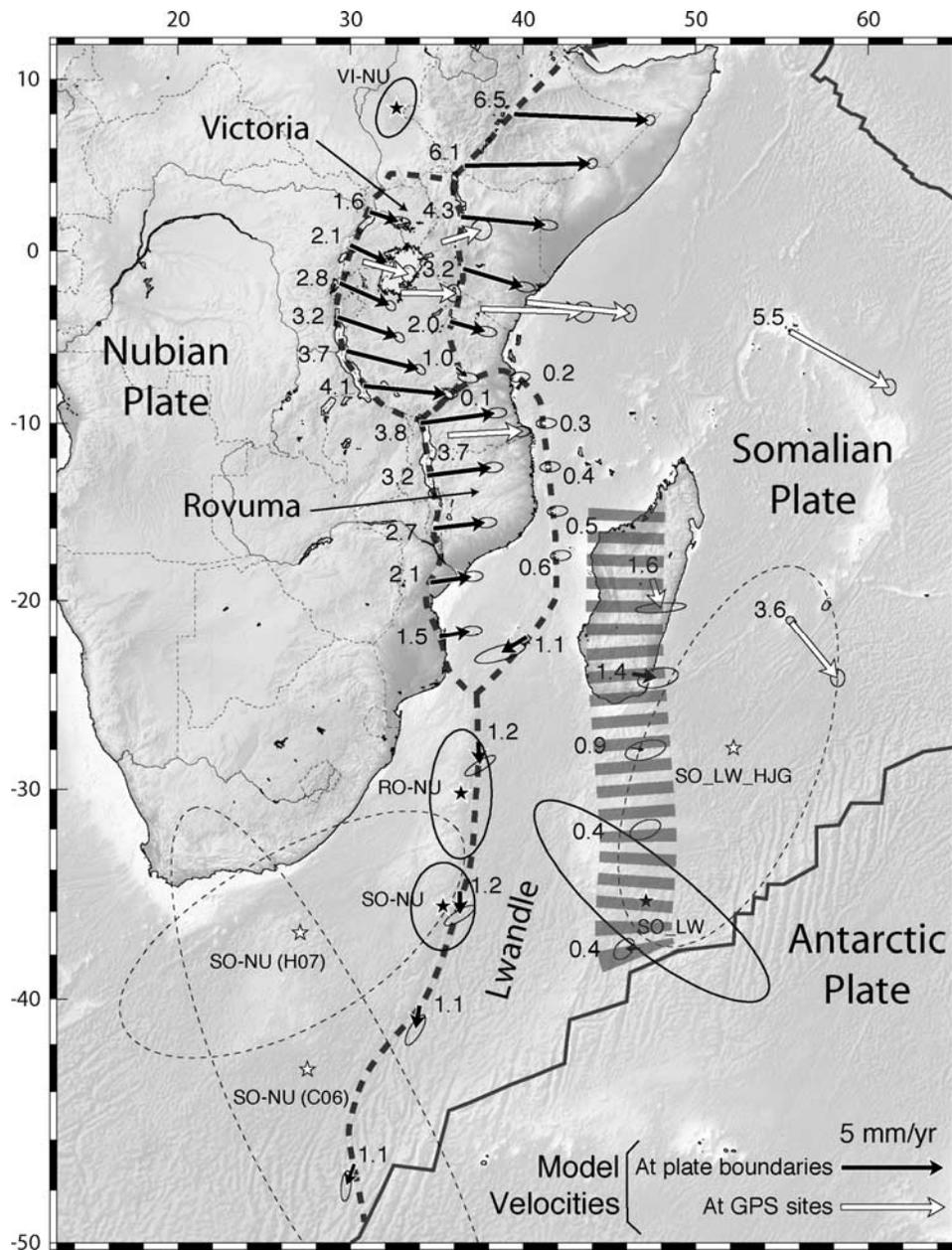
Figure 2. Best-fit model. Relative motions along plate or block boundaries are shown with black arrows, and numbers are model velocities in mm.yr^{-1}. Relative rotation poles are shown with black stars. The first plate rotates counter-clockwise with respect to the second, except for VI-NU where Victoria rotates clockwise with respect to Nubia.

geodetic solution with one more site on the Somalian plate (HIMO) and longer GPS time series.

[19] The Victoria-Nubia angular velocity found here is consistent with the previous estimate by *Calais et al.* [2006] with a significantly reduced uncertainty thanks to a more precise velocity estimate at MBAR and the addition of two new sites on Victoria (ELDS in Kenya and MZA1 in Tanzania). A new GPS velocity at site SNG1 in southern Tanzania allows us to estimate a Rovuma-Nubia rotation pole to the south of the Rovuma plate.

3.3. Tests With a Lwandle Plate

[20] In a second step, we compare two estimates of the Nubia-Somalia-Antarctica relative motions using the same

data set, one without a Lwandle plate and with the geologic data between 29°E and 47°E assigned to the Lwandle-Antarctica segment of the SWIR (as previously), the other with a Lwandle plate and that same geologic data assigned to the Lwandle-Antarctica segment of the SWIR (Table 1). We find that the difference in χ^2 between the two solutions is significant at the 99% confidence level (F = 5.38; Table S1), indicating that the data are fit significantly better by splitting the Lwandle plate from Somalia, as also found by *Horner-Johnson et al.* [2007].

[21] The Lwandle angular velocity from this solution has large uncertainties but predicts (Figure S3) (1) shortening near the southern termination of the eastern boundary of the Lwandle plate, consistent with observed compressional

focal mechanisms at the southern termination of the Madagascar ridge, (2) WNW−ESE directed extension in Madagascar, consistent with earthquake focal mechanisms, field observations [*Kusky et al.*, 2007], and slip vector directions, and (3) SE-directed velocity at site MIR1 on Madagascar, collinear with the observed GPS velocity, although at a rate twice slower. Including earthquake slip vector data in Madagascar and at the southern termination of the Madagascar Ridge reduces the uncertainty of the Lwandle angular velocity (Table 1). The difference in χ^2 between estimates with and without this data set is however not significant (1% probability, F = 0.28). Our best-fit model (Figure 2) has a weighted RMS of 4.2 mm.yr^{-1} for spreading rates, 6.7° for slip vector directions and transform fault azimuths, and 0.6 mm.yr^{-1} for GPS velocities (Figure S3).

[22] Finally, an F-test shows that the χ^2 decrease from an estimate assigning MIR1 to the Lwandle plate to an estimate without MIR1 is significant at the 75% confidence level. The same test with MIR1 on the Somalian plate shows a χ^2 decrease significant at the 80% confidence level. This shows that MIR1 cannot be attributed to either plate with significant confidence and suggests that it lies within the plate boundary zone between Lwandle and Somalia.

4. Discussion

[23] Our estimate of the Somalia-Nubia angular velocity is consistent with that of *Horner-Johnson et al.* [2007] based on 3.2 Myr average oceanic data only. It does not differ significantly if oceanic data along SWIR are included or not in the estimation. This consistency between geologic and geodetic data indicates that the Nubia-Somalia relative motion has remained steady over the past 3 Myr, a result that holds for most major plates [e.g., *Sella et al.*, 2002]. This does not preclude local kinematic changes as the rift structures evolved and the sub-plates identified here formed [e.g., *Ring*, 1994]. Indeed, assuming that present-day extension rates across the central EAR (3 to 6 mm.yr^{-1}) have been constant since the initiation of rifting about 10 Ma years ago, would lead to at least 30 km of cumulative extension. This is more than twice the 15 km maximum finite extension derived from fault geometries [*Ebinger*, 1989], suggesting slower extension rates as rifting initiated.

[24] The plate angular velocities found here predict opening at a rate of 1 to 4 mm.yr^{-1} across the Western and Eastern rifts, increasing from north to south for the former, and from south to north for the latter (Figure 2). This correlates with the age of rifting initiation (from 12− 15 Ma to 8 Ma from North to South along the Western rift and 5 Ma to Present for the Eastern rift [*Ebinger*, 1989]), consistent with a propagation process. The southward decrease of the extension rate along the Eastern branch is consistent with progressive disappearance of prominent active faults, as the Eastern branch propagates into cold cratonic domain. Our model predicts very small motion rate (less than 0.1 mm.yr^{-1}) at the Victoria/Rovuma boundary (a result of their opposite sense of rotation with respect to Nubia), consistent with the limited morphological expression of recent faulting in the Usangu and Ruaha grabens [*Le Gall et al.*, 2004].

[25] The model predicts extension across the Malawi rift at rates decreasing from 4.5 mm.yr^{-1} in the north to 1.5 mm.yr^{-1} at the latitude of the southern Mozambique coastal plain (Figure 2). The Mw = 7.5, 2006, Mozambique earthquake was therefore a rare event, with a long recurrence time (possibly >1,000 years). As along the Eastern branch, the southward decrease of the extension rate from the Malawi rift is consistent with progressive disappearance of prominent active faults and the broadening of the plate boundary zone. Predicted extension rates across the eastern boundary of Rovuma are much lower that along the Malawi rift, ranging from 0.5 to 1 mm.yr^{-1}, consistent with seismic strain release from the 30-year global NEIC catalog.

[26] The Lwandle-Nubia angular velocity is not well determined but predicts right-lateral strike-slip at about 1 mm.yr^{-1} along the poorly known western boundary of the Lwandle plate. In this model, the eastern margin of the Mozambique ridge, which forms a prominent linear step in the bathymetry continuous further south with the Andrew Bain Fracture Zone, is close to a small circle about the Lwandle-Nubia rotation pole. However, no direct observation is available to corroborate active motion along this particular structure. Our model is consistent with (slow) NE−SW shortening at the southern end of the Madagascar ridge and observed E−W extension in Madagascar along the possibly diffuse Lwandle-Somalia plate boundary.

5. Conclusions

[27] Geodetic data on the Nubian, Somalian, and Antarctic plates and earthquake slip vector data along the East African Rift are consistent with 3.2 Myr average spreading rates and transform azimuths along the SWIR and with a kinematic model that includes three plates (Victoria, Rovuma, and Lwandle) between Somalia and Nubia. Predicted motions along active EAR structures are qualitatively consistent with seismicity and active faulting, with extension directions approximately EW but varying spatially as a function of the plates involved. The data used here, therefore, support a rifting model with localized strain along narrow rift structures that isolate large lithospheric blocks. Improved geodetic coverage of Africa and surrounding islands remains, however, essential to test and further refine this kinematic model.

References

Altamimi, Z., X. Collilieux, J. Legrand, B. Garayt, and C. Boucher (2007), ITRF2005: A new release of the International Terrestrial Reference Frame based on time series of station positions and Earth Orientation Parameters, *J. Geophys. Res.*, 112, B09401, doi:10.1029/2007JB004949.

Brazier, R. A., A. A. Nyblade, and J. Florentin (2005), Focal mechanisms and the stress regime in NE and SW Tanzania, East Africa, *Geophys. Res. Lett.*, 32, L14315, doi:10.1029/2005GL023156.

Calais, E., C. J. Ebinger, C. Hartnady, and J. M. Nocquet (2006), Kinematics of the East African rift from GPS and earthquake slip vector data, in *The Afar Volcanic Province Within the East African Rift System*, edited by

G. Yirgu, C. J. Ebinger, and P. K. H. Maguire, *Geol. Soc. Spec. Publ.*, 259, 9–22.

Chu, D., and R. G. Gordon (1999), Evidence for motion between Nubia and Somalia along the Southwest Indian Ridge, *Nature*, 398, 64–67.

Ebinger, C. (1989), Tectonic development of the western branch of the East African rift system, *Geol. Soc. Am. Bull.*, 101, 885–903.

Fenton, C. H., and J. J. Bommer (2006), The *Mw*7 Machaze, Mozambique, earthquake of 23 February 2006, *Seismol. Res. Lett.*, 77, 426–439.

Fernandes, R. M. S., B. A. C. Ambrosius, R. Noomen, L. Bastos, L. Combrinck, J. M. Miranda, and W. Spakman (2004), Angular velocities of Nubia and Somalia from continuous GPS data: Implications on present-day relative kinematics, *Earth Planet. Sci. Lett.*, 222, 197–208.

Foster, A., and J. A. Jackson (1998), Source parameters of large African earthquakes: Implications for crustal rheology and regional kinematics, *Geophys. J. Int.*, 134, 422–448.

Grimison, N. L., and W. P. Chen (1988), Earthquakes in Davie Ridge-Madagascar region and the southern Nubian-Somalian plate boundary, *J. Geophys. Res.*, 93, 10,439–10,450.

Hartnady, C. J. H. (1990), Seismicity and plate boundary evolution in southeastern Africa, *S. Afr. J. Geol.*, 93, 473–484.

Hartnady, C. J. H. (2006), Seismotectonics of southern Mozambique, paper presented at 21st Colloquium on African Geology (CAG21), *Geol. Soc. of S. Afr.*, Maputo, Mozambique.

Horner-Johnson, B. C., R. G. Gordon, S. M. Cowles, and D. F. Argus (2005), The angular velocity of Nubia relative to Somalia and the location of the Nubia-Somalia-Antarctica triple junction, *Geophys. J. Int.*, 162, 221–238, doi:10.1111/j.1365-24X.2005.02608.x.

Horner-Johnson, B. C., R. G. Gordon, and D. F. Argus (2007), Plate kinematic evidence for the existence of a distinct plate between the Nubian and Somalian plates along the Southwest Indian Ridge, *J. Geophys. Res.*, 112, B05418, doi:10.1029/2006JB004519.

Jestin, F., P. Huchon, and J. M. Gaulier (1994), Teh Somali plate and the East African Rift system: Present-day kinematics, *Geophys. J. Int.*, 116, 637–654.

Kusky, T. M., E. Toraman, and R. Raharimahefa (2007), The Great Rift Valley of Madagascar: An extension of the Africa-Somali diffusive plate boundary?, *Gondwana Res.*, 11, 577–579.

Le Gall, B., L. Gernigon, J. Rolet, C. Ebinger, R. Gloaguen, O. Nilsen, H. Dypvik, B. Deffontaines, and A. Mruma (2004), Neogene-Recent rift propagation in central Tanzania: Morphostructural and aeromagnetic evidence from the Kilombero area, *Geol. Soc. Am. Bull.*, 116, 490–510.

Lemaux, J., R. G. Gordon, and J.-Y. Royer (2002), The location of the Nubia-Somalia boundary along the Southwest Indian Ridge, *Geology*, 30, 339–342.

Mougenot, D., M. Recq, P. Virlogeux, and C. Lepvrier (1986), Seaward extension of the East African rift, *Nature*, 321, 399–403.

Nocquet, J. M., P. Willis, and S. Garcia (2006), Plate kinematics of Nubia-Somalia using a combined DORIS and GPS solution, *J. Geod.*, 80, 591–607.

Prawirodirdjo, L., and Y. Bock (2004), Instantaneous global plate motion model from 12 years of continuous GPS observations, *J. Geophys. Res.*, 109, B08405, doi:10.1029/2003JB002944.

Ring, U. (1994), The influence of preexisting crustal anisotropies on the evolution of the Cenozoic Malawi rift (East African rift system), *Tectonics*, 13, 313–326.

Sella, G. F., T. H. Dixon, and A. Mao (2002), REVEL: A model for recent plate velocities from Space Geodesy, *J. Geophys. Res.*, 107(B4), 2081, doi:10.1029/2000JB000033.

Skobelev, S. F., M. Hanon, J. Klerkx, N. N. Govorova, N. V. Lukina, and V. G. Kazmin (2004), Active faults in Africa: A review, *Tectonophysics*, 380, 131–137, doi:10.1016/j.tecto.2003.10.016.

Stein, S., and R. G. Gordon (1984), Statistical tests of additional plate boundaries from plate motion inversions, *Earth Planet. Sci. Lett.*, 69, 401–412.

Willis, P., C. Boucher, H. Fagard, and Z. Altamimi (2005), Geodetic applications of the DORIS system at the French Institut Geographique National, *C. R. Geosci.*, 337, 653–662, doi:10.1016/j.crte.2005.03.002.

―――――――――――

E. Calais and D. S. Stamps, EAS Department, Purdue University, West Lafayette, IN 47907, USA. (dstamps@purdue.edu)

C. J. Ebinger, Department of Geology and Geophysics, University of Rochester, Rochester, NY 14627, USA.

R. M. Fernandes, CGUL, IDL, UBI, R. Marques d'Avila e Bolama, P-6201-001 Covilha, Portugal.

C. Hartnady, Umvoto Africa Ltd., P.O. Box 61, Muizenberg, 7950, Cape Town, South Africa.

J.-M. Nocquet, CNRS Géosciences Azur, Rue Albert Einstein, F-06560 Valbonne, France.

E. Saria, University College for Lands and Architectural Studies, University of Dar Es Salaam, P. O. Box 35176, Dar Es Salaam, Tanzania.